

A Dual-Band Slotted Trapezoidal Inverted-F Antenna for Indoor WLAN Communications

Feng Pang^{1, 2}, Jungang Yin^{3, *}, Wei Chen³, Jian Yang⁴, Chao Xie³, and Xiang Li³

Abstract—This letter presents a new directional dual-band slotted trapezoidal inverted-F antenna (IFA) for indoor Wireless Local Area Network (WLAN) applications. The dual-band performance can be obtained by tuning the lengths of the inner symmetrical trapezoidal slots and the outer trapezoidal arms in a nearly independent manner. The measured results show that the proposed antenna can provide two separate impedance bandwidths (return loss better than 10 dB) around 180 MHz and 750 MHz for 2.4/5.1–5.8 GHz WLAN bands, respectively. Good radiation performance and roughly constant in-band antenna directivities are also observed.

1. INTRODUCTION

Multiband or wideband antennas have increasingly attracted great attention in the wireless industry as so many different wireless technologies are developed rapidly. A large number of antennas have been designed for wireless local area network (WLAN) applications [1–5]. Most of them have omnidirectional radiation patterns applied to wireless terminals, such as mobiles, pads, and laptops. For indoor wireless access points or point-to-point communications, however, it is often required that the antenna is somewhat directional to allow the installation of the antenna against a wall or on a ceiling surface [6–8]. Slotted structures are often used to realize multi-band performance [9–11], in particular for dual-band patches [12, 13]. One resonance is due to the fundamental mode of the main patch, while the currents along slot edges introduce an additional resonance.

In this letter, we present a new directional dual-band slotted trapezoidal planar inverted-F antenna, with low profile and low manufacture cost, and capable of covering the 2.4/5.1–5.8 GHz dual WLAN bands for indoor communications.

2. ANALYSIS AND SIMULATION

The geometry of the proposed dual-band slotted trapezoidal inverted-F antenna is presented in Fig. 1. The proposed antenna has been simulated and optimized by using *CST MWS*. The simulated surface current distribution shown in Fig. 2 implies that a dual-band performance can be obtained by tuning the two inner symmetrical trapezoidal slots and the outer trapezoidal arms.

The lower and upper resonance frequencies are primarily related to length l_1 of the inner slots and length l_2 of the outer arms, and can be approximated by the following empirical expressions based on the simulations, in a similar format as in [14]:

$$f_L \approx \frac{c}{2 \times (3 \times l_1)} \quad (1)$$

$$f_H \approx \frac{c}{2 \times l_2} \quad (2)$$

Received 13 October 2016, Accepted 15 November 2016, Scheduled 29 November 2016

* Corresponding author: Jungang Yin (jg.yin@hnu.edu.cn).

¹ National Astronomical Observatories of Chinese Academy of Sciences, Beijing 100012, China. ² University of Chinese Academy of Sciences, Beijing 100049, China. ³ Department of Electronics at Hunan University, Changsha 410082, China. ⁴ Department of Signals and Systems at Chalmers University of Technology, Gothenburg, S-412 96, Sweden.


$$l_1 \approx \frac{h_1}{\sin \theta} - \frac{d_2}{\sin \theta} + d_1 - w_1 \quad (3)$$

c is the light speed in free space, and f_L and f_H are the lower and upper resonance frequency, respectively.

A parameter sweeping for S_{11} performance over all parameters included in Eqs. (1)–(4) has been carried out. It is found from Figs. 4–8 that the resonance tips over both the lower and upper bands tend to be sensitive to parameters h_1 and d_2 . However, h_2 and θ affect the S_{11} tip primarily in the upper band but hardly in the lower band. In contrast, d_1 affects the S_{11} tip primarily over the lower band but little over the upper band. In other words, the variation of h_1 and d_2 affects the S_{11} performance over both the lower and upper bands; the changes of d_2 and θ affect the performance only in the lower band while d_1 affects the performance only in the upper band. Consequently, the antenna geometry can be designed in such a scheme that h_1 and d_2 are first tuned to roughly fix the dual-band, while h_2 , θ and d_1 are then fine-tuned to improve the S_{11} performance in dual bands in a nearly independent manner.

The optimized geometrical parameters are listed in Table 1. As can be seen, its total size is $47.0 \times 35.0 \times 4.5 \text{ mm}^3$, which is much thinner than that ($43 \times 26 \times 12 \text{ mm}^3$) of a 2.4/5.8 GHz dual-band directional antenna proposed in [8] for RFID reader applications, and much more compact than that ($57 \times 57 \times 21 \text{ mm}^3$) of a 2.5–4.8 GHz slot antenna designed for WLAN systems in [10].

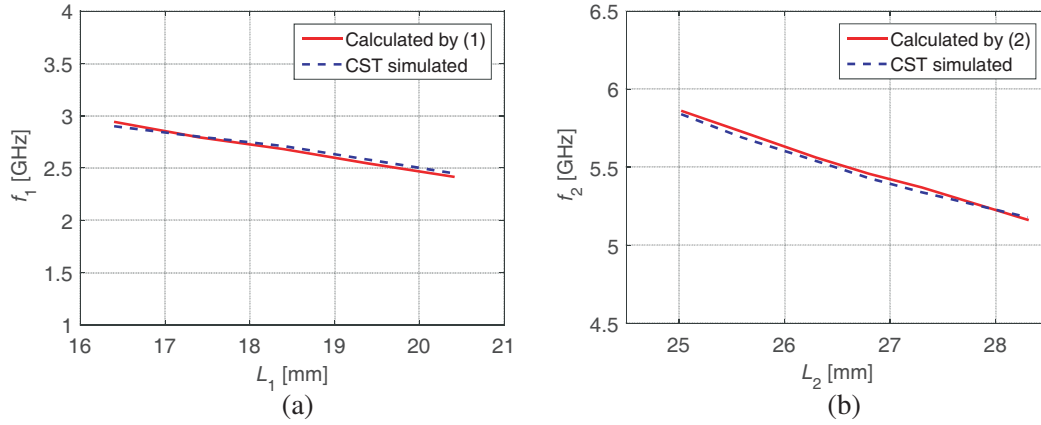


Figure 3. Comparisons of resonance frequency between calculations by expressions (1)–(2) and CST simulations: (a) f_L ; (b) f_H .

Table 1. Geometric parameters of the proposed antenna.

Parameter	Value	Parameter	Value
S	23.0 mm	w_1	1.0 mm
H	4.5 mm	w_2	3.0 mm
W	35.0 mm	w_3	3.2 mm
L	47.0 mm	d_1	6.0 mm
θ	63.0°	d_2	0.0 mm
h_1	13.8 mm	d_3	11.5 mm
h_2	18.5 mm	t	0.1 mm

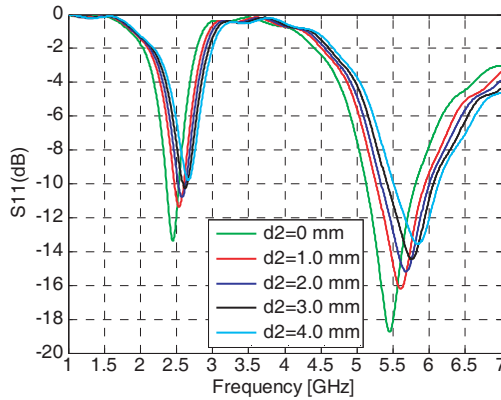


Figure 4. Sweeping of d_2 for S_{11} while other parameters set as in Table 1.

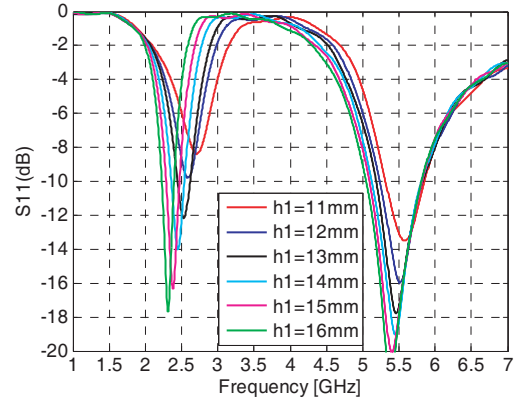


Figure 5. Sweeping of h_1 for S_{11} while other parameters set as in Table 1.

3. MEASURED RESULTS

As can be seen in Fig. 9, the fabricated trapezoidal inverted-F antenna is made of copper and probe-fed through an air cavity by an SMA connector, which is in low-profile, low-cost and easy to fabricate.

The measured and simulated reflection coefficients of the proposed antenna are demonstrated in Fig. 10. The measured bandwidth defined by return loss better than 10 dB (10 dB impedance bandwidth) is around 180 MHz (2.41–2.59 GHz) and 750 MHz (5.01–5.76 GHz) at dual bands, respectively. It is observed that the measured results agree very well with the simulated ones. The slight deviation is

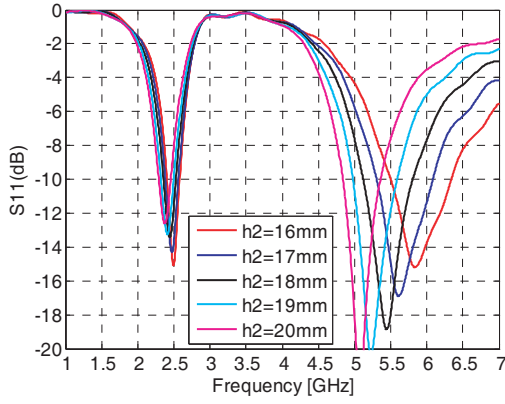


Figure 6. Sweeping of h_2 for S_{11} while other parameters set as in Table 1.

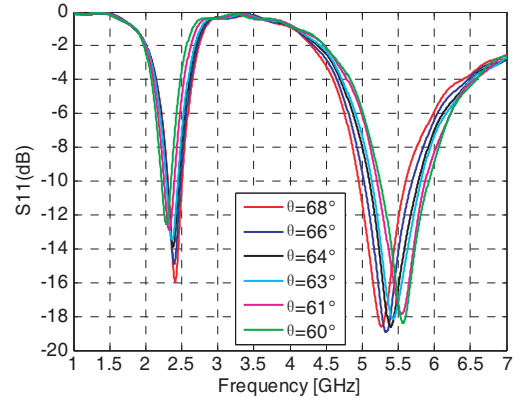


Figure 7. Sweeping of θ for S_{11} while other parameters set as in Table 1.

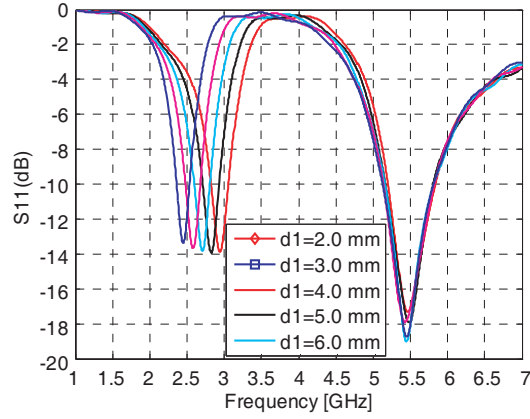


Figure 8. Sweeping of d_1 for S_{11} while other parameters set as in Table 1.

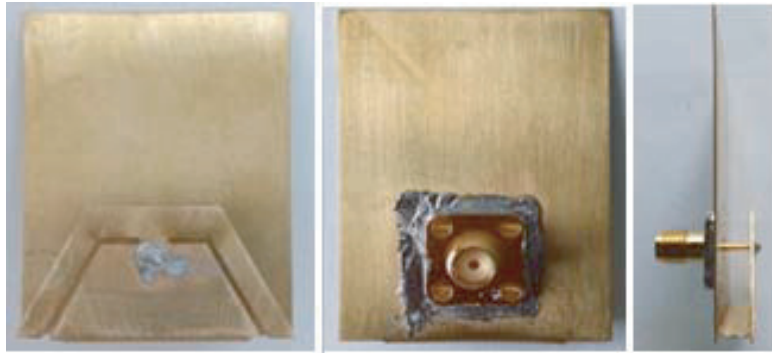


Figure 9. Top/bottom/side view of the fabricated antenna prototype.

due to the tolerances, deformation and soldering, which cause some perturbation to the cavity. The measured 10 dB bandwidths are sufficiently large to fully cover the dual WLAN bands.

The far-field patterns were measured in an anechoic chamber with the Agilent antenna-measurement system. The measured E - and H -plane co-polar patterns at 2.44/5.2/5.5/5.8 GHz are displayed in Fig. 11.

Listed in Table 2 are the measured co-polar directivities at certain frequency points in the lower and upper bands. The simulated and measured co-polar directivities in the upper band are shown in

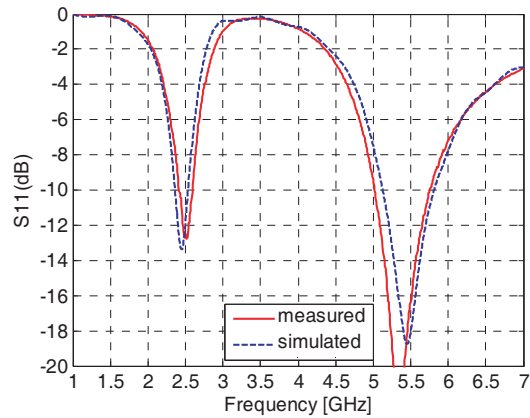


Figure 10. Simulated and measured S_{11} parameters of the proposed antenna.

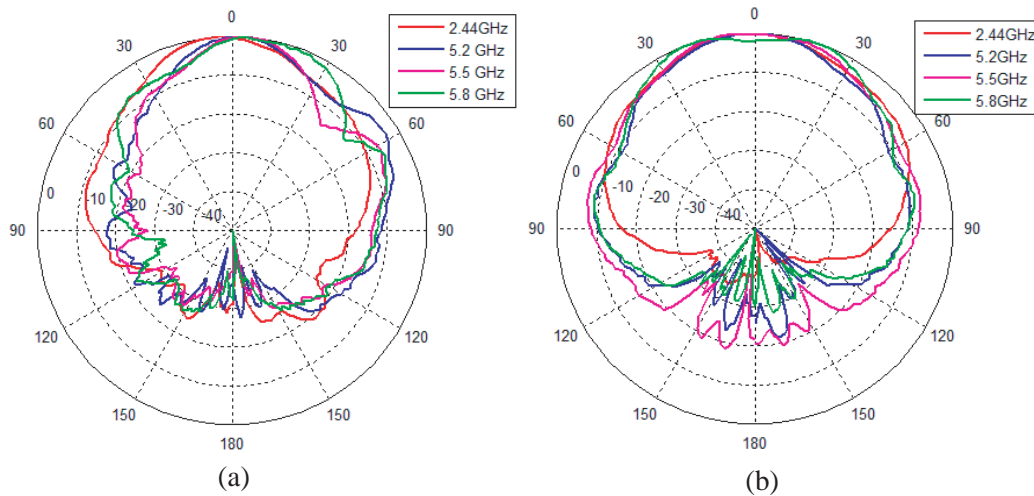


Figure 11. Measured co-polar patterns in (a) E -plane and in (b) H -plane at different frequencies.

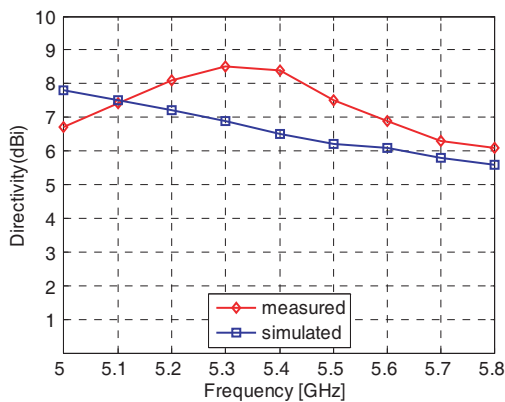


Figure 12. Measured and simulated antenna directivities in upper band.

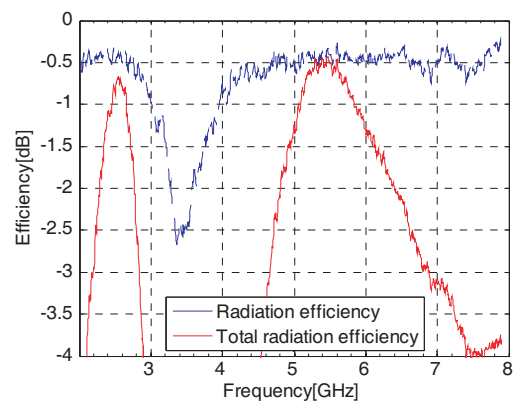


Figure 13. Measured radiation efficiencies over the dual bands.

Fig. 12. It can be seen that the directivities vary from about 6.1 to 8.3 dBi between 5.1 and 5.8 GHz, and good agreement is observed between the measured and the simulated results. The deviation is due to accessories for measurement setup, such as the supporting plate, poles, screws, and cables.

Table 2. Measured directivities in dual bands.

Frequency (GHz)	Directivity (dBi)	Frequency (GHz)	Directivity (dBi)
2.40	6.1	5.10	7.2
2.44	5.7	5.50	7.5
2.50	6.0	5.80	6.1

The radiation efficiency of the antenna prototype, which is a measure of its ohmic losses, as well as the total radiation efficiency that takes both its ohmic and mismatch losses into account, was measured in a Blue test reverberation chamber [15], where the measurement uncertainty is 0.5 dB [16]. The measured data were obtained by using a rigorous calibration method presented in [17]. It can be observed from Fig. 13 that the measured radiation efficiency is about -0.5 dB over both the lower and upper bands; the measured total radiation efficiency is higher than -0.7 dB over the upper band, while it is higher than -1.0 dB over the lower band, due to a bit worse matching performance in the lower band than that in the upper band.

4. CONCLUSION

A new directional dual-band slotted trapezoidal inverted-F antenna is proposed and studied in this letter. The simple formulas as design guidelines for the dual resonance frequencies are provided. The measurement results of the prototype agree well with the simulation ones. About 180/750 MHz bandwidths defined by return loss better than 10 dB are obtained at 2.4–2.5/5.1–5.8 GHz WLAN bands, respectively. Around 6.0 dBi directivities are observed at the lower band and 6.1–8.3 dBi at the upper band. The measured total radiation efficiencies are better than -0.7 dB over the upper band and better than -1.0 dB over the lower band. Besides, the proposed antenna is in low-profile, low-cost and easy to fabricate, making it ready to be applied in indoor WLAN communications.

ACKNOWLEDGMENT

This work was supported by Chinese Ministry of Science and Technology under grant No. 2013CB837900, by National Natural Science Foundation of China under grant Nos. 11261140641 and 11503049, by Chinese Academy of Sciences under grant No. KJZD-EW-T01, and by Hunan University under the Youth Researcher Growth Program.

REFERENCES

1. Kuo, Y.-L. and K.-L. Wong, "Printed double-T monopole antenna for 2.4/5.2 GHz dual-band WLAN operations," *IEEE Trans. Antennas Propag.*, Vol. 51, No. 9, 2187–2192, Sep. 2003.
2. Jan, J.-Y. and L.-C. Tseng, "Small planar monopole antenna with ashorted parasitic inverted-L wire for wireless communications in the 2.4, 5.2 and 5.8-GHz bands," *IEEE Trans. Antennas Propag.*, Vol. 52, No. 7, 1903–1905, Jul. 2004.
3. Wong, K.-L., L.-C. Chou, and C.-M. Su, "Dual-band flat-plate antenna with a shorted parasitic element for laptop applications," *IEEE Trans. Antennas Propag.*, Vol. 53, No. 1, 539–544, Jan. 2005.
4. Zhang, H. and H. Xin, "A dual-band dipole antenna with integrated balun," *IEEE Trans. Antennas Propag.*, Vol. 57, No. 3, 786–789, Mar. 2009.
5. Shih, Y.-K., W.-J. Liao, S.-H. Chang, P.-C. Chiang, C.-T. Yeh, and T.-G. Ma, "A four element antenna system with antenna diversity for dual band WLAN operation," *Proceedings of 2013 URSI International Symposium on Electromagnetic Theory (EMTS)*, 679–682, May 2013.
6. Gardelli, R., G. La Cono, and M. Albani, "A low-cost suspended patch antenna for WLAN access points and point-to-point links," *IEEE Antennas Wireless Propag. Lett.*, Vol. 3, 90–93, 2004.

7. Medeiros, C. R., E. B. Lima, J. R. Costa, and C. A. Fernandes, "Wideband slot antenna for WLAN access points," *IEEE Antennas Wireless Propag. Lett.*, Vol. 9, 79–82, 2010.
8. Quan, X., R. Li, Y. Cui, and M. M. Tentzeris, "Analysis and design of a compact dual-band directional antenna," *IEEE Antennas Wireless Propag. Lett.*, Vol. 11, 547–550, 2012.
9. Huang, C.-Y. and E.-Z. Yu, "A slot-monopole antenna for dual-band WLAN applications," *IEEE Antennas Wireless Propag. Lett.*, Vol. 10, 500–502, 2011.
10. Zhang, N., P. Li, B. Liu, X. W. Shi, and Y. J. Wang, "Dual-band and low cross-polarisation printed dipole antenna with L-slot and tapered structure for WLAN applications," *Electron. Lett.*, No. 47, 360–361, 2011.
11. Row, J.-S., "Dual-frequency triangular planar inverted-F antenna," *IEEE Trans. Antennas Propag.*, Vol. 53, No. 2, 874–876, 2005.
12. Huynhand, T. and K. F. Lee, "Single-layer single-patch wideband microstrip antenna," *Electron. Lett.*, Vol. 31, 1310–1312, Aug. 1995.
13. Row, J.-S., "Dual-frequency triangular planar inverted-F antenna," *IEEE Trans. Antennas Propag.*, No. 53, 874–876, 2005.
14. Liu, Z. D., P. S. Hall, and D. Wake, "Dual-frequency planar inverted-F antenna," *IEEE Trans. Antennas Propag.*, Vol. 45, 1451–1458, 1997.
15. Bluetest, A. B., <http://www.bluetest.se>.
16. Kildal, P.-S., X. Chen, C. Orlenius, et al., "Characterization of reverberation chambers for OTA measurements of wireless devices: Physical formulations of channel matrix and new uncertainty formula," *IEEE Trans. Antennas Propag.*, Vol. 60, No. 8, 3875–3891, 2012.
17. Raza, H., J. Yang, and A. Hussain, "Measurement of radiation efficiency of multiport antennas with feeding network corrections," *IEEE Antennas Wireless Propag. Lett.*, Vol. 11, 89–92, 2012.